

CHAPTER 28

3-D Salt and Overthrust Seismic Models

Fred Aminzadeh*

Aminzadeh, F., 3-D salt and overthrust seismic models, in P. Weimer and T. L. Davis, eds., AAPG Studies in Geology No. 42 and SEG Geophysical Developments Series No. 5, AAPG/SEG, Tulsa, p. 247-256.

ABSTRACT

We have designed two 3-D geologic models and simulated realistic 3-D surveys based on those models. This has been a collaborative effort of the Society of Exploration Geophysicists (SEG), the European Association of Exploration Geophysicists, and the United States Department of Energy National Laboratories. The project is usually referred to as the SEG/EAEG Modeling, or SEM, project. The two salt and overthrust 3-D models and the respective synthetic datasets will be made available to both the oil industry and academia. This SEM project has been a sizable undertaking, with computational requirements of several million dollars. By the end of 1995, about 800 gigabytes of data had been generated, completing Phase A and Phase B of the project. "Classic datasets" containing subsets of calculations conducted for Phases A and B have been defined. Any other subsets of data could be extracted from the whole dataset using a procedure devised at Lawrence Livermore National Laboratory (LLNL). Additional calculations of about three terabytes, Phase C, will be carried out as the project is completed around mid-1997. These datasets have already been used by many for testing and validating processing algorithms and aiding in survey design. Their use as standard 3-D datasets is expected to increase for many years.

INTRODUCTION

Three-dimensional model data are useful for testing 3-D processing algorithms (e.g., migration, velocity analysis, multiple suppression), understanding wave propagation in a complex 3-D medium, choosing proper acquisition parameters, and testing various data compression and data transmission techniques. They can also be used for training as well as benchmarking different hardware platforms.

Examples of models that have gained widespread popularity for various types of testing and benchmarking are the 3-D French model (French, 1974) and the 2-D Marmousi model (Lailly and Versteeg, 1990). In recent years, advances in computer technology have enabled bigger problems to be modeled. This capability, combined with the ever-increasing complexity of the structures that are being explored and developed, has necessitated construction of more complicated 3-D models.

After a number of surveys of the SEG membership and discussions during various workshops, we have made final decisions on different aspects of the 3-D models. Some of the issues that had to be decided were:

- structural/stratigraphic nature of the model,
- model representation,
- acquisition parameters,
- numerical techniques for generation of seismograms,
- model type (acoustic vs. elastic), and
- computer resources requirements and contributors.

Given the constraints of available computer resources and the immediate needs of the industry, the following compromises had to be made:

- (1) Structural problems are the main focus of this modeling effort, although the overthrust model includes some stratigraphic features (channel sand).
- (2) Geological models are represented using University of Nancy's GOCAD Project software.
- (3) Acquisition parameters are decided in different phases of the project based on the available resources.
- (4) Marine acquisition geometry is used for both models to avoid land topography problems.
- (5) The finite difference method is used for calculations.
- (6) The calculations are based on an acoustic medium.
- (7) Computer resources of the U.S. National Laboratories are used to construct the model responses.

Two acoustic models were chosen to carry out the simulation: a salt dome model with features similar to those of the U.S. Gulf of Mexico and an overthrust model that was a 3-D extension of the earlier 2-D Marmousi model. Working groups were formed to finalize separate details of the project, such as (1) construction of the Overthrust Model, (2) construction of the Salt Dome Model, and (3) selection and porting of the finite differences codes to different platforms and execution of the numerical computations.

Other working groups have been formed to help finalize the survey parameters and to develop a scheme for storing and distributing large volumes of the numerical calculations. For other background information and more details about the evolution of this project, refer to Aminzadeh et al. (1994a, 1994b, 1995, 1996) and Kunz et al. (1995).

SALT DOME MODEL

The design of the salt model was accomplished through the participation of 27 representatives (experienced in salt tectonics, seismic modeling, and seismic imaging) from 23 organizations representing oil companies, seismic contractors, and academia. It was agreed by these representatives to base the salt model on a typical Gulf Coast salt structure. Special care was taken to ensure both its geological reasonability and its adequacy as a testing mechanism for seismic

*Unocal Corporation, 14141, SW FWY, Sugar Land, TX 77487

imaging algorithms (particularly subsalt).

Figure 1 shows the 3-D perspective of the salt model with the salt sill, different faults, sand bodies, and lenses. The salt model exhibits the following major features: (1) a north-westwardly plunging stock; (2) a secondary reactivation crest, located southward of the stock; (3) a broad, low-relief eastern flank; (4) a faulted southern flank with minor toe thrust; and (5) a rounded overhang on the west flank. The northern flank is bounded by a counterregional fault, with attendant downthrown rollover structure in the outboard section. Two down-to-the-basin faults occur beneath the salt sill; one offsets the salt base. The salt edge crosscuts stratigraphy at a low angle and varies in shape around the sill perimeter. The eastern flank exhibits a mildly downturned edge. The southern flank exhibits an upturned edge; the western flank has a rounded edge; and the northeastern edge of the salt contains a salt weld. The overall model dimensions are $13.5 \times 13.5 \times 4.2$ km in the x, y, and z directions, respectively. The maximum sill length is approximately 9.5 km, and the maximum sill width is approximately 6.6 km. The salt crest is at approximately 325 m.

The model contains five sands, some of which are gas charged. At least one sand will contain both a gas/oil and an oil/water contact. The two shallowest sands truncate against the sill base. One of the intermediate sands is stratigraphically isolated, and the other conforms to the subsalt anticline. The model contains a shale sheath that is modeled to be geopressured. The seafloor (bathymetry) map exhibits a counterregional fault scarp and a bathymetric rise associated with the sill crest. The map also exhibits a shelf break at the southeast end of the model.

This model is designed in part to be able to test various imaging algorithms in different geologic settings: salt flank, salt overhang, and subsalt. The velocity model is generated using a 20-m grid with 15-Hz center frequency for the wavelet. The velocities surrounding the salt body are typical of Gulf of Mexico sediments and are described by compaction gradients based on (K, V_0) curves (V_0 is the initial velocity, and K is the velocity gradient that varies spatially) and a geopressure surface. The following expression is used to define the 3-D velocity field:

$$V(x,y,z) = V_0 + z K(x,y) - GP, \quad (1)$$

where GP is the deceleration term for velocities below the geopressure surface. The water and salt velocities and GP are chosen to be 1500, 4481, and 46 respectively. Figure 2 shows another 3-D display of the model with two perpendicular 2-D velocity profiles. Three parallel cross sections from the three dimensional velocity grid of Figure 2 are depicted in Figure 3. Color velocity scales to the right of Figure 3 are in meters per second, with blue indicating the high salt velocities. Green color indicates relatively lower sediment velocities of the overpressure zones.

We make a constant-density assumption due to the limitations of the finite difference code. The model also contains five point diffractors and a flat horizon above the model basement, which may be used as a means of evaluating the quality of seismic imaging algorithms. Since the constant density assumption and the simple velocity gradient structure given by Equation 1 result in no reflectivity in the sediment surrounding the salt, we use the “spike” method to create reflections from geologic boundaries. This method increases the velocity of the function for each successive layer as shown in Figure 4. As shown in Figure 5, the synthetic seismogram of the AA' cross section of Figure 3 exhibits proper reflections from geologic boundaries using the spike velocity profile of Figure 4.

OVERTHRUST MODEL

A complex thrusted sedimentary succession has been constructed on top of a structurally decoupled extensional and rift basement block. The thrust unit has been built from a collection of 2-D balanced cross sections. Figure 6 shows a 3-D perspective of the overthrust model. The basement (not shown) underneath the overthrust structure includes an extensional fault block system, with a sediment cover on the basement blocks. Above this, there is an erosional truncation, and there is a structural uncoupling between basal and uppermost units. A petroleum trap has been introduced between the two reverse faults in the heavily folded thrust. Also observe the sand channel included in the west side of the model. Figure 7 shows the original 2-D cross sections that were used in constructing the 3-D overthrust model. The model represents two converging thrusts plus an additional blind thrust which dies out laterally. The faults in the overthrust and the basement have been validated by the Fault Analysis Group of the University of Liverpool. The model is overlain by a flat sedimentary layer underneath the seabed. Figure 8 shows various cross sections of the overthrust model. The model has dimensions of $20 \times 20 \times 3.5$ km, giving a zone of maximum seismic coverage of $10 \times 10 \times 3.5$ km. In total, it has 17 layers. The model presents varying degrees of complexity, with a central thrust-faulted anticline and an external monocline and flat zone. The top of the overthrust is eroded and covered by a surface layer to represent recent sediments. Channels and crevasse splay lenses are present in some layers. The layer thickness is preserved, and the percentage shortening at any point across the thrust structure is approximately constant. Fault planes have been checked by 3-D visualization to ensure smoothness and regularity. Figure 9 shows the process by which fault rifts were built by the fault analysis group of the University of Liverpool.

The basement of the overthrust model is composed of alternating layers of carbonate and siliciclastic sedimentary rocks which drape tilted, extensional fault blocks. There is a petroleum trap in the tilted strata draping the middle block. The upper boundary of this extensional unit is an erosional truncation. This layer is in turn overlain by a sedimentary succession in which an initial salt layer is overlain by predominantly marine sedimentary stratigraphy composed of two major carbonate successions and siliciclastic and argillaceous sediments. The salt layer acts as decollement surface for two thrust planes which deform the upper sediment column. The lower of the two thrusts converges laterally with the upper plane. The layers in the area bounded by the faults are folded into an anticline with a fold axis that varies laterally to create a closed petroleum trap in the sandstone layer. The folds contain reverse limbs at the point of minimum structural depth. There is a bulge in the footwall of the thrust sequences that dies out laterally. The thrust layers are capped by a thin sedimentary veneer and a sea layer. Several constructive criticisms on the model have been provided by various companies, the major recommendations being:

- The model should be an onshore rather than an offshore structure, with substantial topography and a complex weathering zone.
- The model should include even more 3-D properties.
- The velocity distribution should be constructed from an existing database.
- Some features (imbrication of thin beds, lenses, pinchouts, etc.) should be included to address the problem of seismic resolution.

While these points are all valid, the choices made were mostly constrained by the available computational resources and the limitations of the code chosen based on various other considerations.

COMPUTATIONS AND THE 3-D FINITE DIFFERENCE CODE

We concluded early on that 3-D structural problems should be the primary focus of this effort. Because extensive wave propagation computations through an elastic medium in a survey-size setting is still beyond reach of today's technologies, a full-sized seismic survey will therefore be limited to acoustic computations only.

Several 3-D finite difference (FD) codes have been provided by various organizations for acoustic wave propagation computations in the 3-D model. The Computation Working Group conducted extensive evaluations of these candidate codes. The FD 3-D wave propagation code provided by the Institut Francais du Petrole (IFP), with a second-order scheme in time and a tenth-order scheme in space, was chosen for the entire simulation. The time steps are 1 ms, while the space steps (x, y, z) are 25 m. The parallel version of this code is implemented on different supercomputers: Paragon, Meiko CS-2, Cray Research c-916, Connection Machine CM-5, and Fujitsu VP 2400. The entire calculation is divided into segments to be carried out on various machines located in different laboratories. For this reason, extensive work was done to ensure that different platforms would yield the same results.

These calculations are done under the Department of Energy (DOE) Gas and Oil National Information Infrastructure (GONII) project. Four national laboratories—Lawrence Livermore, Los Alamos, Oak Ridge, and Sandia—are contributing to these efforts. Aside from computation, resources and technologies available at the national laboratories, such as networking, high-speed I/O, mass data storage, collaborative tools, distributed computing, visualization, and computer security, are being used to increase the utility of this project to the oil industry.

SALT CALCULATION

The Phase A acquisition program for the salt model contains two perpendicular lines which span the model with a shot spacing of 80 m. Each of these lines is a broad-line swath across the model. Figure 10 shows the orientation of these lines and the receiver grid pattern for shot line 1. Each line has 138 shots. In addition, two downhole shots were calculated at depth locations of 900 and 2300 m at a vertical well located at the intersection of the two lines. All Phase A calculations (total of 278 shots) have been completed. The data have been stored on the on-line storage system at LLNL.

The Phase B acquisition program for the salt model contains 35 shot lines which span the model with a shot spacing of 320 m. All of the lines are broad-line swaths across the model. In Figure 11, the large square with the coarse grids displays the acquisition geometry. In total, Phase B represents a coarse source spacing 3-D survey across the entire model. The two wells in the salt model are included whenever the wells are within the computational grid. All Phase B calculations have been completed, and the data now reside on the on-line storage system at LLNL.

Phase C plans for the salt model are expected to increase number of total shots by a factor of four. The acquisition for Phase C consists of infilling Phase B shots within a selected

area of the model so the resulting shots have an 80-m shot spacing inline and a 160-m shot spacing crossline (Figure 11). The selected area contains 24 shot lines, each containing 25 shots from phase B. To infill these shots to an 80-m spacing inline will require an additional 1728 shots. To reduce the crossline shot spacing to 160 m will require an additional 25 shot lines. Each of these new shot lines is offset 40 m in the inline direction from the Phase B lines to simulate a typical marine acquisition. Phase C will use 97 shots from Phase A, 600 shots from Phase B, and an additional 4103 shots that still need to be acquired. Figure 11 shows the two crossing shot lines from Phase A, in yellow and green, and the coarse shots from Phase B. The Phase C infill shot lines are displayed in yellow, and the new shot lines for Phase C are shown in purple. To be consistent with shots previously acquired, the new shots for Phase C will be acquired using the 279×279 receiver geometry used in Phases A and B. As can be seen in Figure 11, Phase C provides dense 3-D shot coverage over the stem, crest, and toe rollers of the salt.

OVERTHRUST CALCULATION

Overthrust calculations were also done in two phases, A and B. Plans for additional calculations are underway. Figure 12 shows the acquisition geometry for Phases A and B and two components of Phase C (C1 and C2).

Phase A (539 shots) was done along the shot line on Figure 12. Figures 13 and 14 show a sample 3-D shot over the overthrust model and the respective time slices of the wave propagation through the model. Phase A results allow comparisons between 2-D and 3-D processing for dip and strike lines. In addition, data corresponding to different well acquisitions are recorded to study well-to-surface seismic ties in a 3-D complex area. Phase A consists mainly of two lines :

- a dip line, 15.55 km long, with a shot interval of 50 m, and
- a strike line, covering 10 km, with an intershot spacing of 50 m.

In addition, data corresponding to various well acquisitions are recorded to study well-to-surface seismic tie in a 3-D complex area.

- A set of 52 wells is located along the dip line to record normal-incidence VSPs. The first well is located at $X = 700$ m; the wells are spaced 300 m apart. The receivers are located from top to bottom (4000 m) in each well with a vertical spacing of 50 m. The objective is to help the interpretation of the surface seismic events.
- A large 2-D walk-away (VSP) is recorded during the computation of the dip line shots.

Phase B (1767 shots) corresponds to a coarse source spacing 3-D acquisition over an area of 15×10.2 km (Figure 12). These data cover most of the structures of the model, in particular the anticline thrust limited by the two main faults. This phase consists of a set of shot lines in the dip direction, with a line spacing equal to 600 m.

Phase C (1620 shots) contains two parts. Phase C1 is a dense 3-D survey over a small portion of the model with a shot spacing of 100 m in both the x and y directions. Phase C1 covers the intersection of the two main faults of the Overthrust Model. Phase C2 completes the Phase B acquisition pattern and leads to a more realistic simulated land 3-D survey with 100 m between shots and 600 m between shot

lines over the whole area of 15×10.2 km surveyed in Phase A and Phase B of the acquisition program. See Figure 12 for details.

LLNL'S FAST STORAGE FACILITY FOR THE SEM DATASET

Lawrence Livermore National Laboratory (LLNL) has developed tools for accessing more than one terabyte of modeling data. This SEM dataset (SEMD) resides at LLNL's FAST storage facility. Because of the massive size of the modeling project data, tools for easily extracting useful subsets of data are crucial. Four distinct methods for doing these extractions are being pursued: classic datasets, web-based forms, an X-Windows-based tool, and an SEG-P1 parser.

The first three methods will be accessed via the World-Wide Web (WWW). The easiest option for the user will be to download directly from a set of predefined "classic" datasets extracted from the SEMD. These classic datasets, which are interesting subsets of data culled from the project data, are defined next.

For users wanting to build their own subsets of the SEMD, a Website for selecting the model, lines, and seismic traces of interest is provided. Once the selection has been made, the requested data will automatically be extracted from the FAST storage system and sent to the requester in the desired format on the Internet. Interactive searching, browsing, and downloading of the project data can be accomplished using the SEMD home page, <http://WildCat.ocf.llnl.gov/SSD/> on the World-Wide Web.

A more sophisticated X-based graphical interface to SEMD extraction will also be provided. This tool will allow the user to set up a virtual seismic survey on either the salt or the overthrust model data. The user will be able to control all aspects of the shot and receiver layout. The result of this operation will be a reasonable sized collection of traces, which will be automatically extracted from the appropriate shot files in the storage facility.

The final method for extracting data from the modeling project data will be a program which uses the shot and receiver information from a user-provided SEG-P1 file to drive the data extraction process. The SEG-P1 file is an industry standard file which contains seismic survey details. This method allows investigators to use their favorite survey tools to define the shot and receiver locations. The same low-level data extraction tools used by the X-based graphical interface described earlier will be employed by this method for creating the subsets. Figure 15 shows a menu for selecting the desired subsets of SEMD.

CLASSIC DATASETS

To provide industry and academia with manageable, consistent, and useful subsets of the SEM dataset, several classic datasets (CDS) have been defined. These datasets will be made available upon request. The following are the CDS for the salt model. Similar CDSs are being defined for the overthrust model. In the near future, access to these datasets will be provided through the Internet.

PHASE A CLASSIC DATASET 0-CDS A0

This is composed of a raw shot gather at grid node 384,441 with a square of 279×279 receivers. In addition, it includes a simulation of 3-D plane wave source (zero-offset

data). The sample interval is 8 ms; the recording time is 5 s. The total dataset size is approximately 193 mb. This location is at the intersection of Phase 1, Line 1 and Phase 2, Line 2 at the crest of the salt.

PHASE A CLASSIC DATASET 1-CDS A1

This is Line 1 (the yellow line on Figure 10) with 138 shots simulating a six-streamer marine acquisition with 65 groups per streamer. The group interval is 40 m, near offset is 160 m, and far offset is 2760 m. The sample interval is 8 ms and the recording time 5 s. The dataset size is approximately 133 mb. CDS A2 is the same as CDS A1, except it contains the blue line on Figure 10, perpendicular to line 1, as described earlier.

PHASE B CLASSIC DATASET 1-CDS B1

This dataset includes selected shots from Phase 2. It contains 156 shots of streamer marine acquisition with 65 groups per streamer. The group interval is 40 m, the near offset is 160 m, and the far offset is 2760 m. The sample interval is 8 ms and the recording time 5 s. The dataset is approximately 150 mb.

Other classic datasets for specific applications (e.g., velocity analysis) are under development.

SOME PRELIMINARY APPLICATIONS

The following important preliminary experimentation has already been done with these models.

PSEUDO-VSP GENERATION

An overthrust model shot gather has been used to test a new idea for generating a pseudo-VSP section by Alai et al. (1995). This tool has proven to be useful in understanding the nature (multiple or primary) and the origination point of different events on a seismic trace. Figure 16A shows a dip section of the velocity volume of the SEM model where the vertical line depicts the location of the gather, or "well." Figure 16B shows a slice through the migrated volume that images the sand channel. Using the velocity profile of Figure 16C and a slice of the shot record of Figure 16E, the pseudo-VSP section shown in Figure 16D is generated. This section helps establish the relationship between events in the original gather and migrated section.

CAN WE IMAGE BELOW SALT?

O'Brien and Gray (1996) uses the AA' 2-D velocity profile shown in Figure 3 and the corresponding "exploding reflector" zero-offset section of Figure 5 to answer this question. They conclude that the SEM data provide the necessary challenge for improving the imaging software. In addition, other processing issues, such as multiple elimination techniques, can be tested using these SEM models. For example, Figure 17 shows O'Brian and Gray's final imaging result after elimination of surface multiples and limiting the range of the data to 0–8000 ft (2438 m).

GULF OF MEXICO SUBSALT SEISMIC IMAGING PROJECT

The Gulf of Mexico Subsalt Seismic Imaging Project was initiated under the Cooperative Research and Development Agreement (CRADA) LA94C1051, between the DOE and several oil companies. Under this project, an exploding

reflector modeling experiment has been performed using the SEMD and the data have been migrated using the salt model velocity grid of SEM. Figures 18 and 19 show some of the migration results. Figure 18 shows the match between the original model surfaces and the migrated events. In this figure, we see a thin sand lens below salt and only the top portion of a second sand layer, also below salt. In Figure 19 we see the event imprint of two thin lenses on a depth section. These results are encouraging in that we see that it is possible to image events below salt in the SEM.

CONCLUSIONS

The SEM project goal has been to design two 3-D models, salt and overthrust, and simulate realistic 3-D surveys over these complicated structures through numerical calculations. The datasets generated through this project in four national DOE laboratories will be made available to industry and academia. Many groups have already begun using and testing the datasets for various applications. In addition, a new umbrella Advanced Computational Technology Initiative (ACTI) project has been initiated to enhance the value of the SEM effort by developing and testing new modeling, processing, and analysis tools using the results of SEM as its basis. See House et al. (1996) for more detail. The strong support and involvement of industry at different stages of the SEM project has been a key to its success up to this point. We expect increased utilization of these datasets over the next several years, especially as Phase C data become available.

Acknowledgments

This has been a truly collaborative effort with contributions from the oil industry, academia, and national laboratories. I would like to specially thank Tim Kunz of Amoco, Kay Wyatt of Phillips Petroleum, Fabien Bosquet of Gocad, Laurence Niccoliti and Pierre Duclos of IFP, Norm Burkhard of Lawrence Livermore National Laboratory, and Fabio Rocca of Politecnico di Milano who have made significant contributions during the course of this project.

REFERENCES CITED

- Alai, R., W. E. A. Rietveld, C. P. A. Wapenar, and A. J. Berkhouit, 1995, From seismic surface measurements to pseudo VSP data: a new tool in 3-D seismic interpretation: Proceedings of SEG-Rio Conference, August.
- Aminzadeh, F., F. Rocca, K. Wyatt, P. Lailly, and N. Burkhard, N., 1994a, Progress report from the SEG/EAEG 3-D Modeling Committee: The Leading Edge of Geophysics, v. 13, n. 2, p. 105–109.
- Aminzadeh, F., N. Burkhard, L. Nicoletis, F. Rocca, and K. Wyatt, 1994b, SEG/EAEG modeling committee project: 2nd report: The Leading Edge of Geophysics, v. 13, n. 9, p. 137–145.
- Aminzadeh, F., N. Burkhard, T. Kunz, L. Nicoletis, and F. Rocca, 1995, 3-D modeling project: 3rd report, The Leading Edge of Geophysics, v. 14, n. 2, p. 125–128.
- Aminzadeh, F., N. Burkhard, J. Long, T. Kunz, and P. Duclos, 1996, Three dimensional SEG/EAEG models, an update: The Leading Edge of Geophysics, v. 15, n. 2, p. 131–134.
- French, W. S., 1974, Two-dimensional and three-dimensional migration of model experiment reflection profiles: Geophysics, v. 39, p. 265–277.
- House, L., M. Fehler, F. Aminzadeh, J. Barhen, and S. Larsen, 1996, A national laboratory-industry collaboration to use SEG/EAEG model data sets.: The Leading Edge of Geophysics, v. 15, n. 2, p. 135–136.
- Kunz, T., F. Bosquet, and F. Aminzadeh, 1995, Constructing and visualizing the SEG/EAEG salt models: Proceedings of Archie Conference on Visualization Technology to Find More Oil and Gas, May 14–18, 1995, The Woodlands, TX.
- Lailly, P., and R. Versteeg, 1990, Marmousi model, Proceedings of the EAEG Research Workshop.
- O'Brien, M. J., and S. H. Gray, 1996, Can we image beneath salt?: The Leading Edge of Geophysics, v. 15, n. 1, p. 17–22.

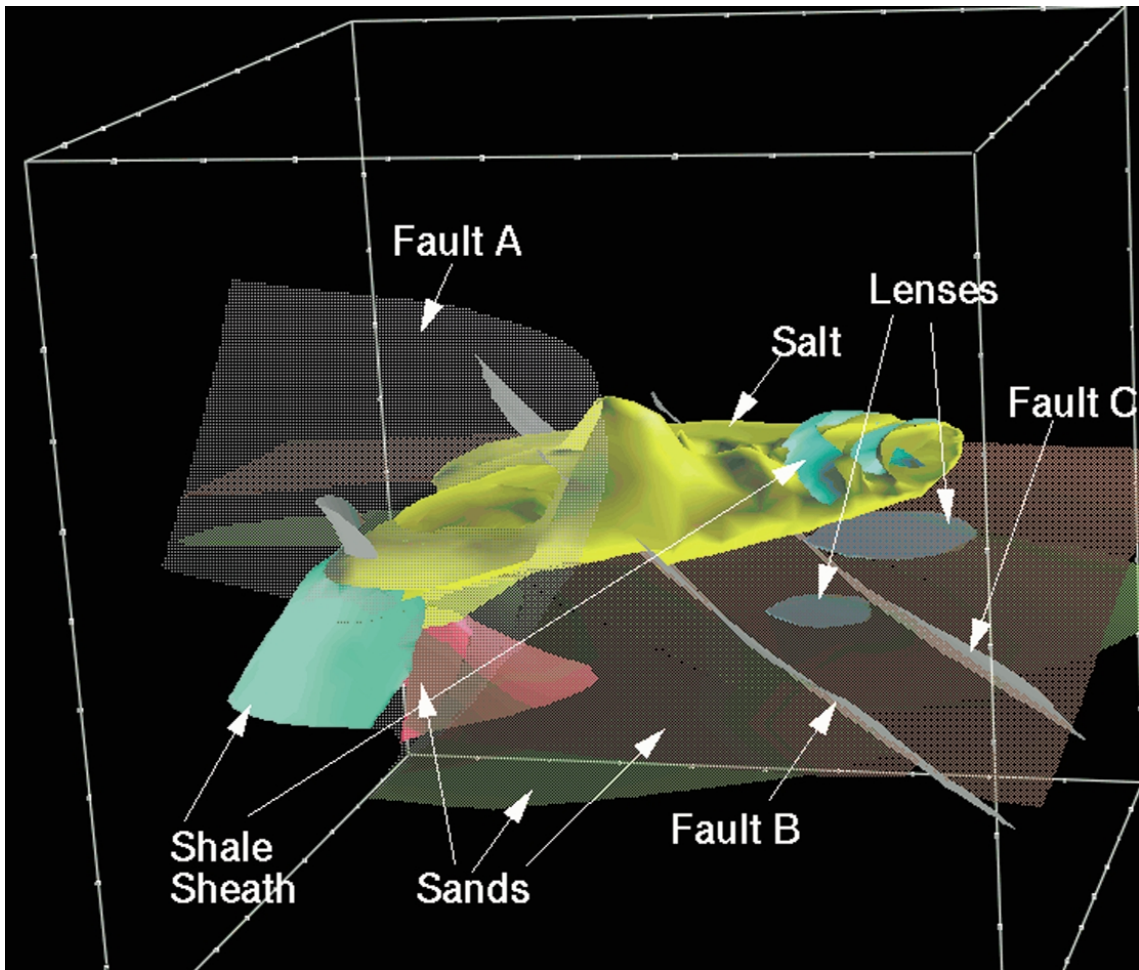


FIGURE 1. The 3-D perspective of the salt model.

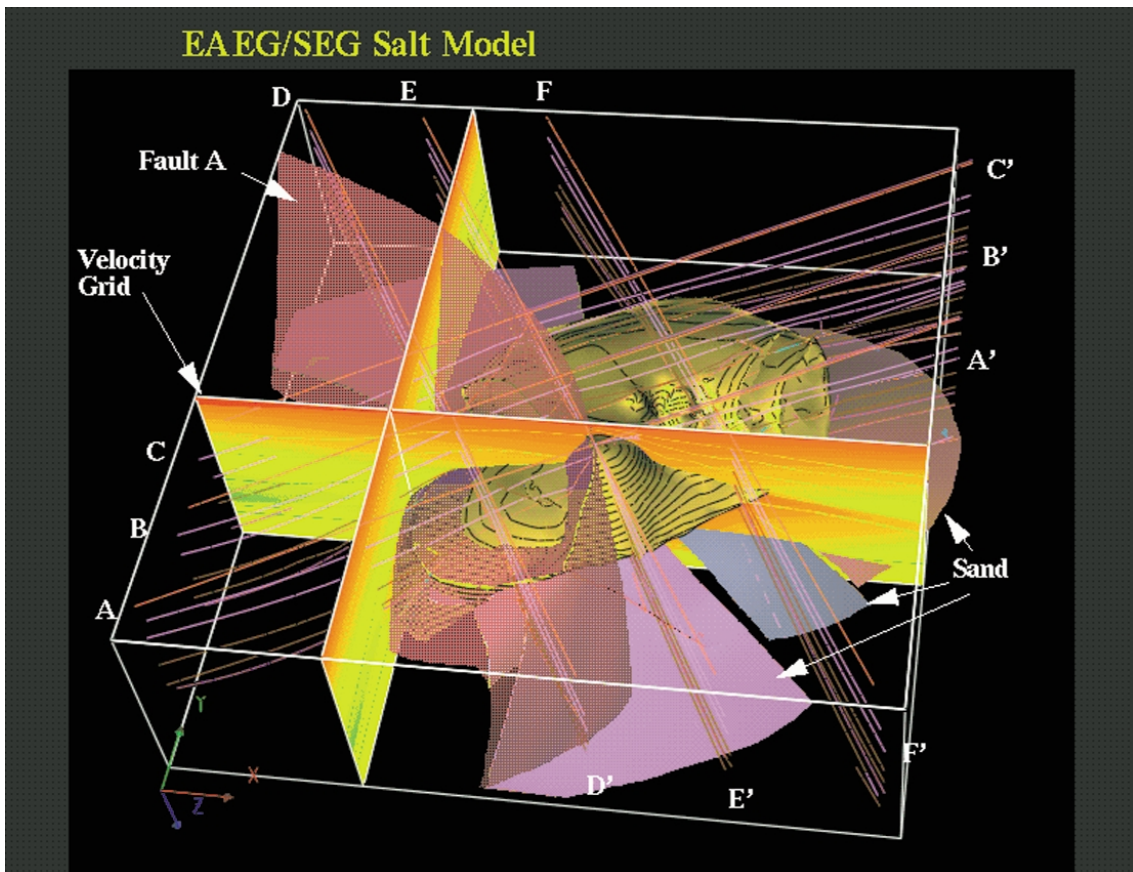


FIGURE 2. The salt model with two velocity profiles.

3 Parallel Cross-Sections

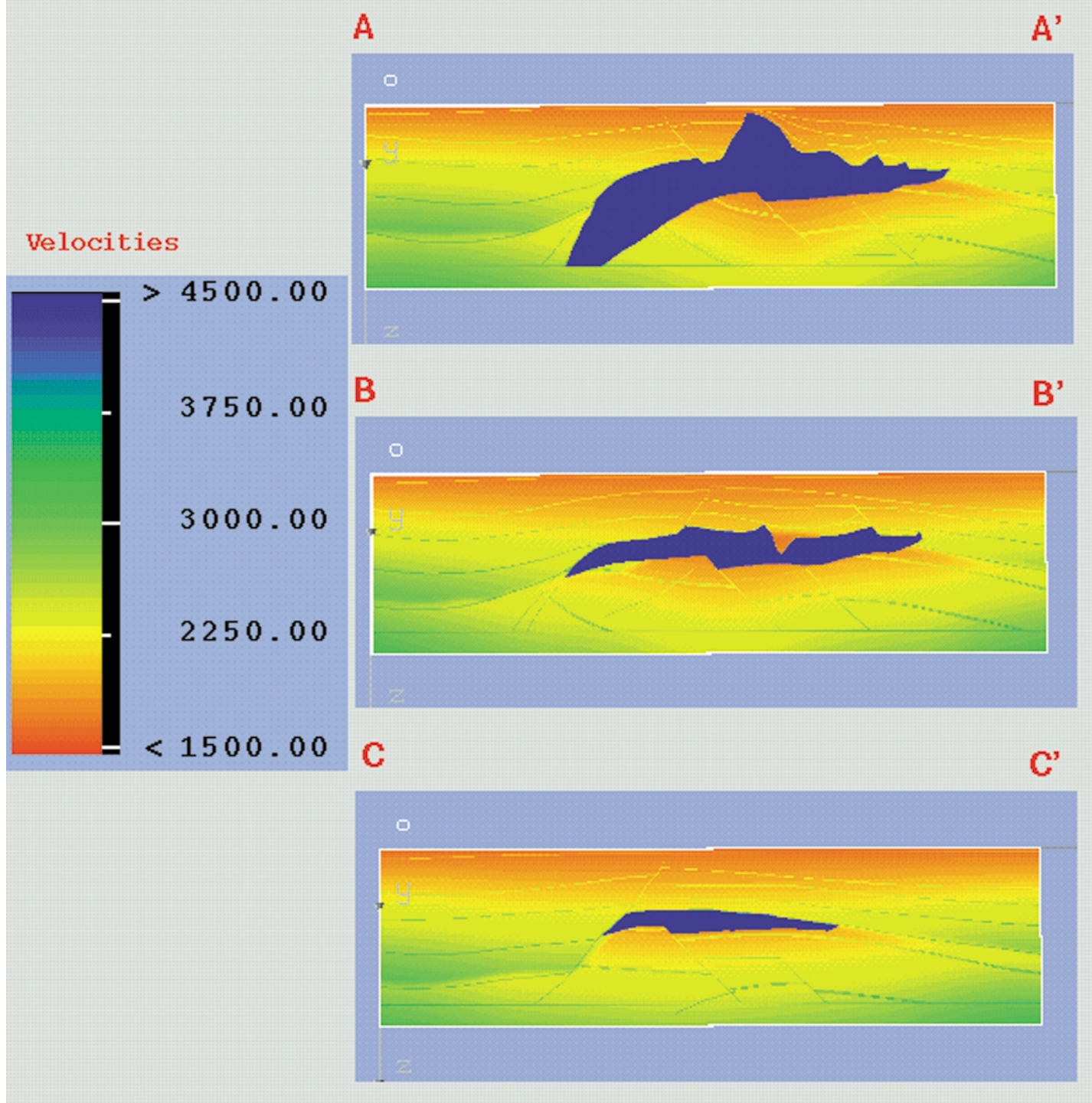


FIGURE 3. Velocity profiles on three parallel cross sections.

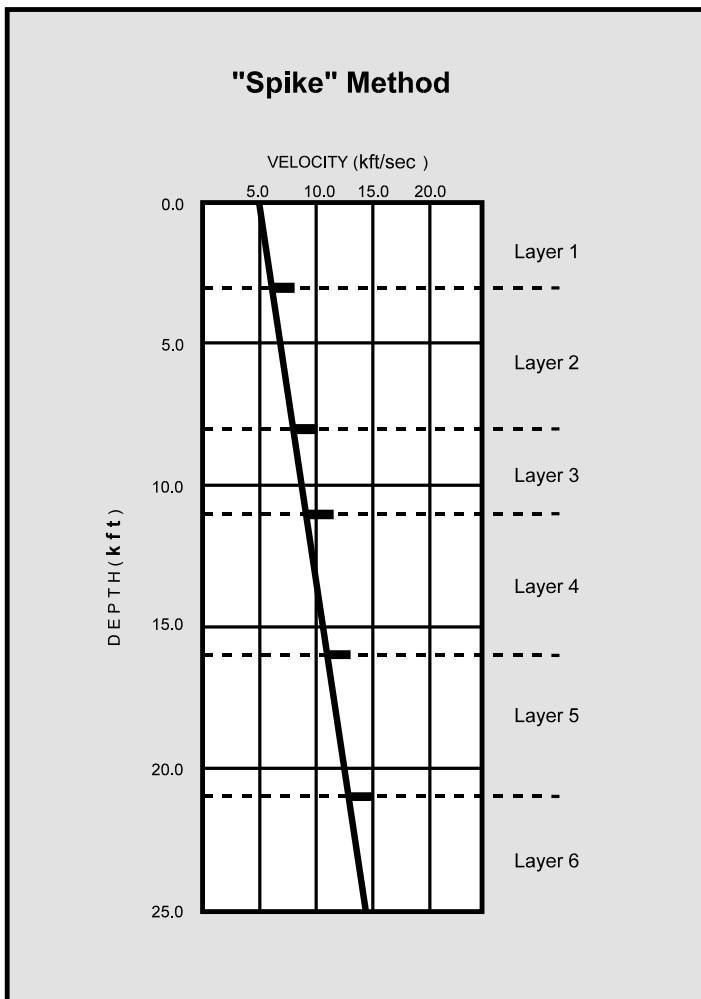


FIGURE 4. Velocity profile using the "spike" method.

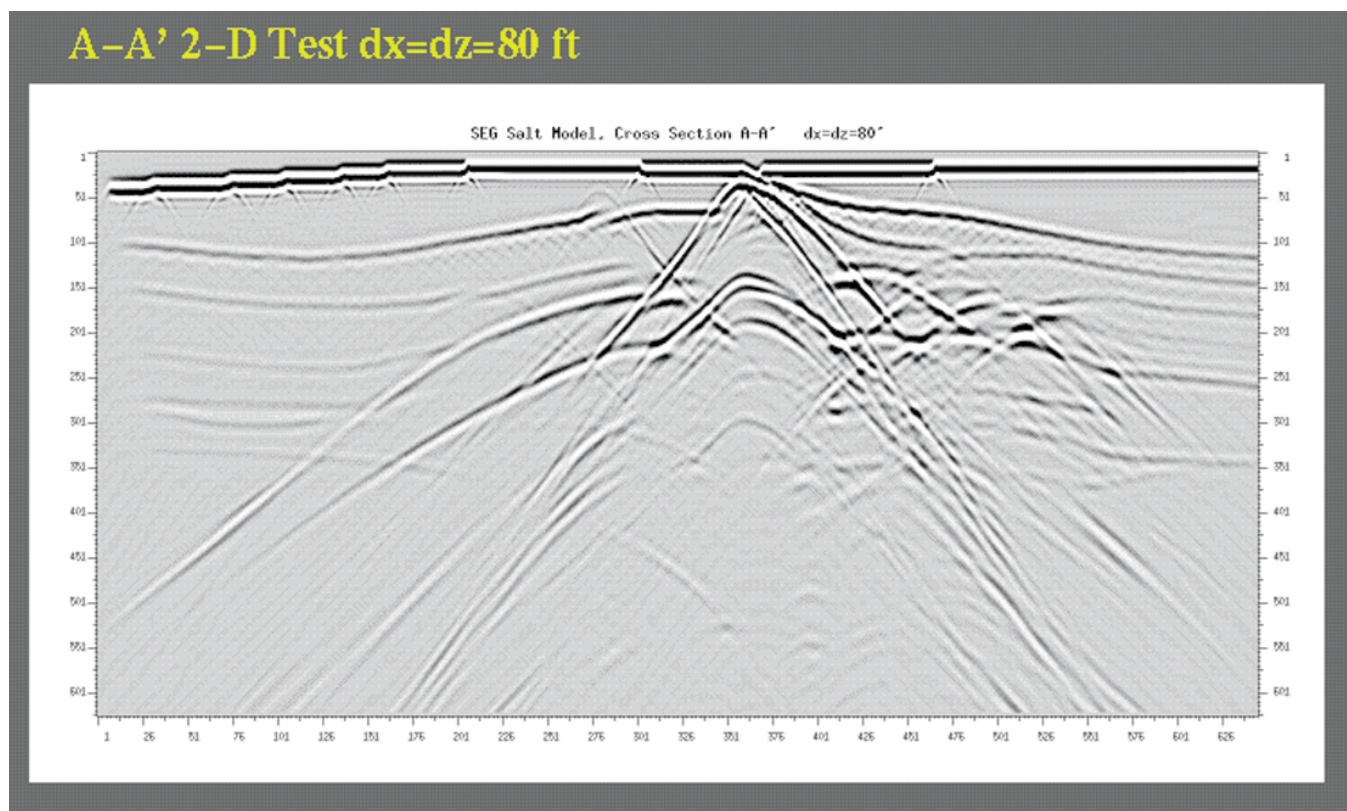


FIGURE 5. 2-D synthetic seismogram of the AA' cross section.

Overthrust Model

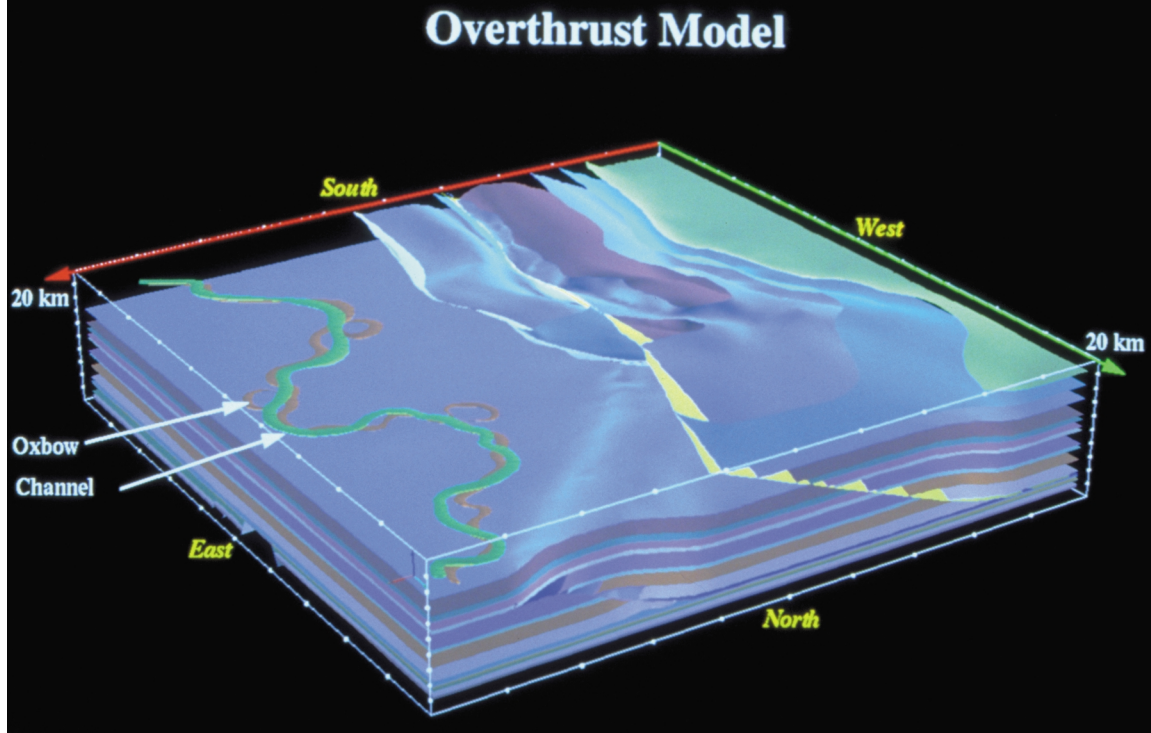


FIGURE 6. The 3-D perspective of the overthrust model.

Cross-Section Data Set

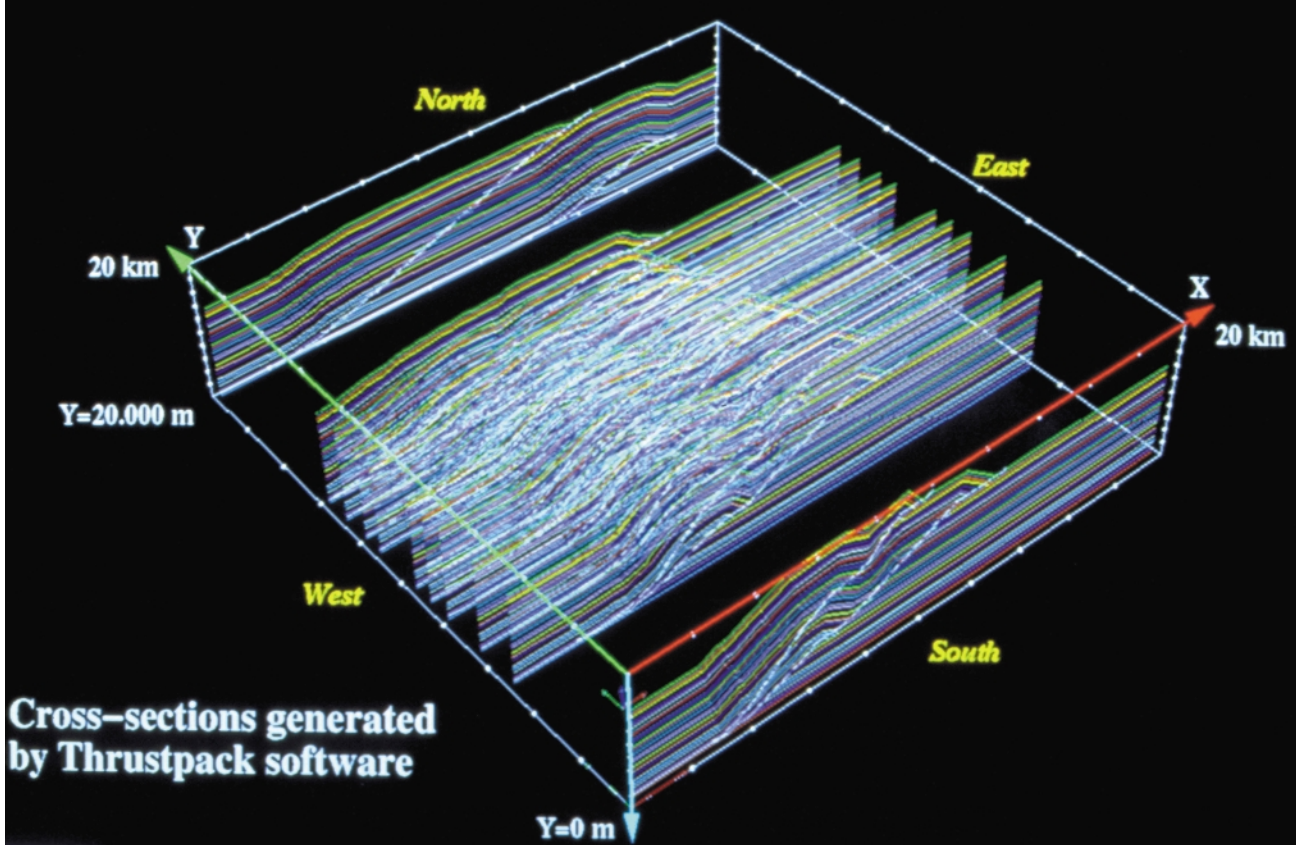


FIGURE 7. Cross section dataset used to generate the 3-D overthrust model.

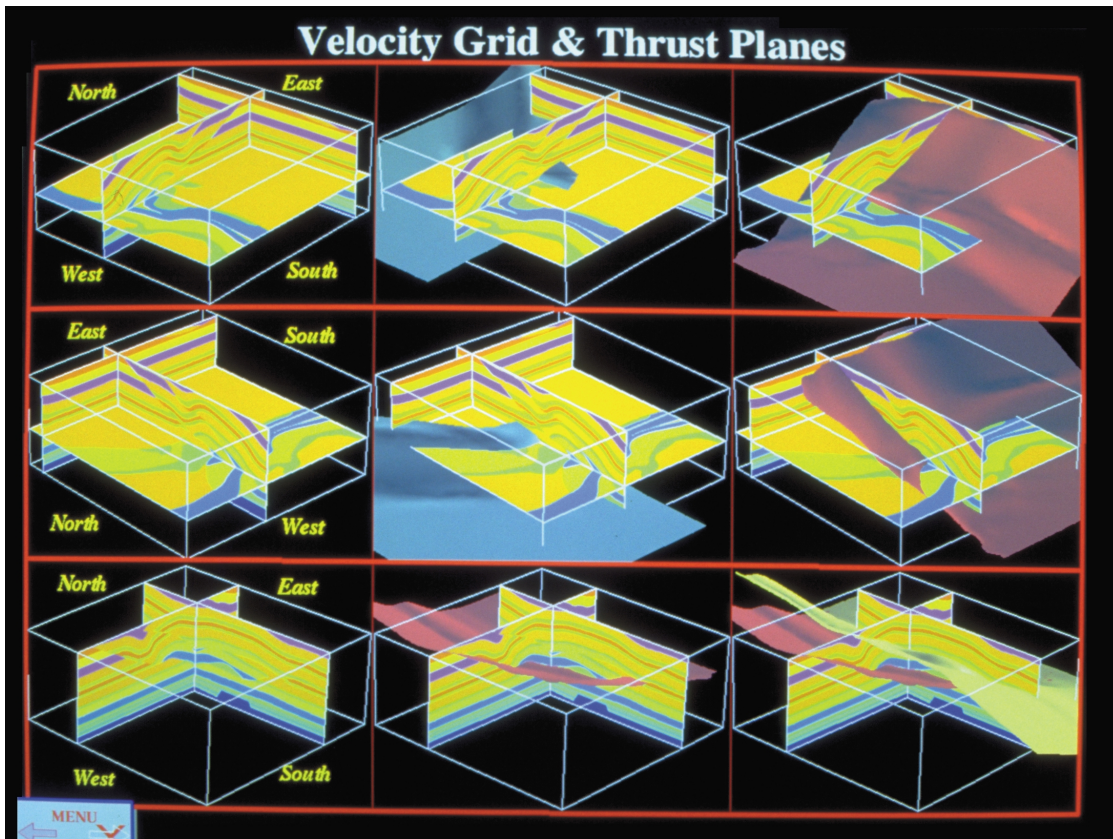


FIGURE 8. 2-D slices through the overthrust model, showing the respective positions of the thrust planes.

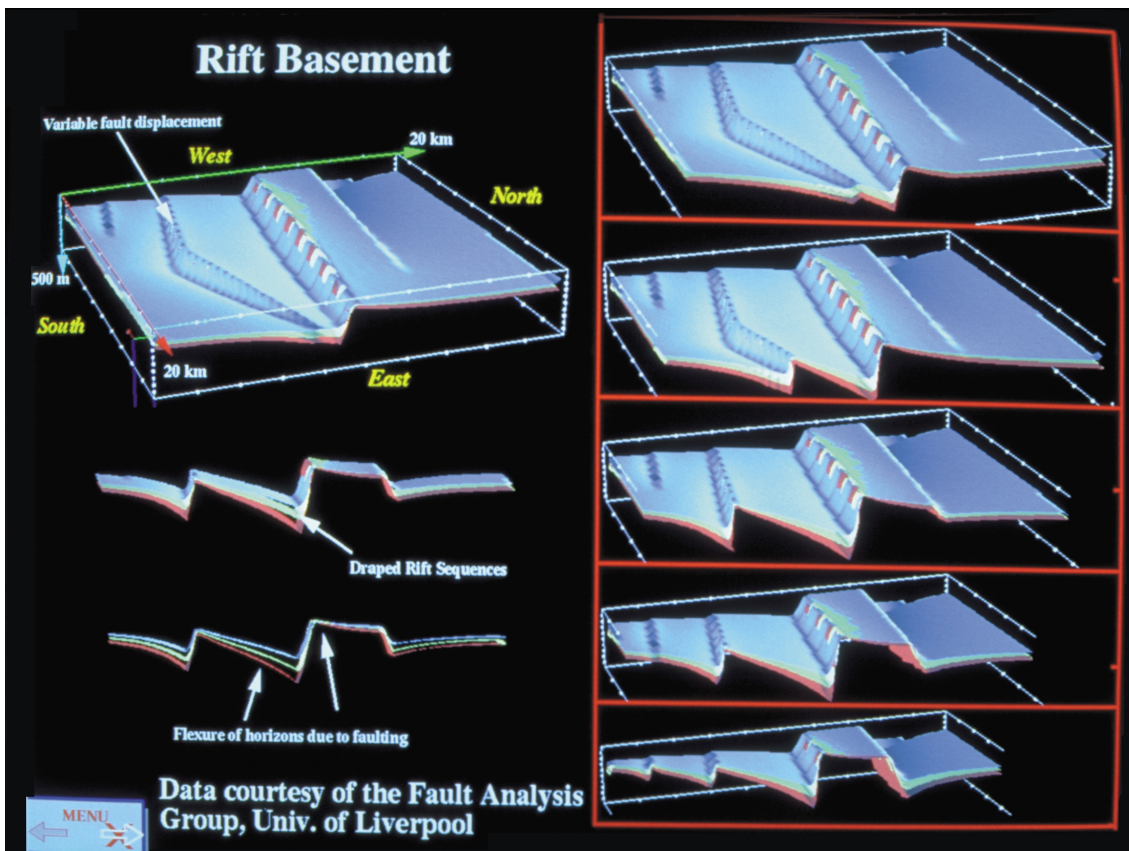


FIGURE 9. Building of the fault planes. (Courtesy of fault analysis group, University of Liverpool.)

Phase 1 Shot Line 1

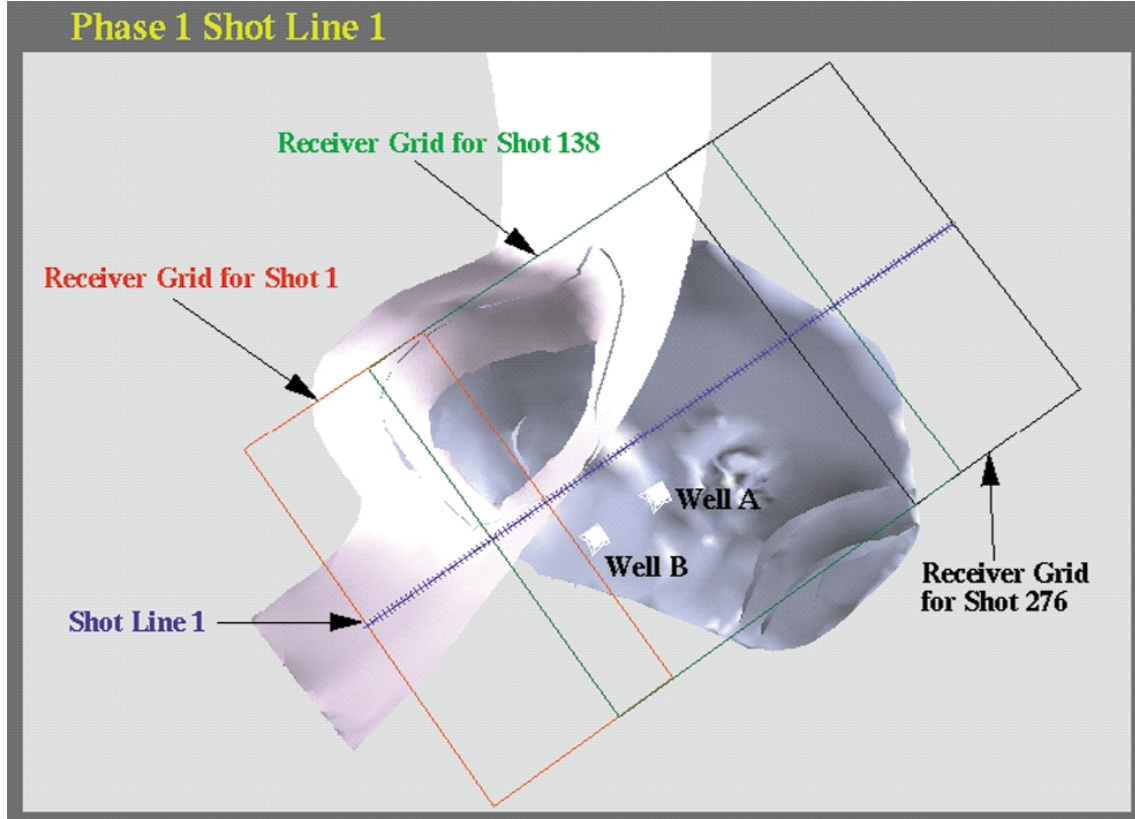


FIGURE 10.
Orientation of two
lines for phase A cal-
culations.

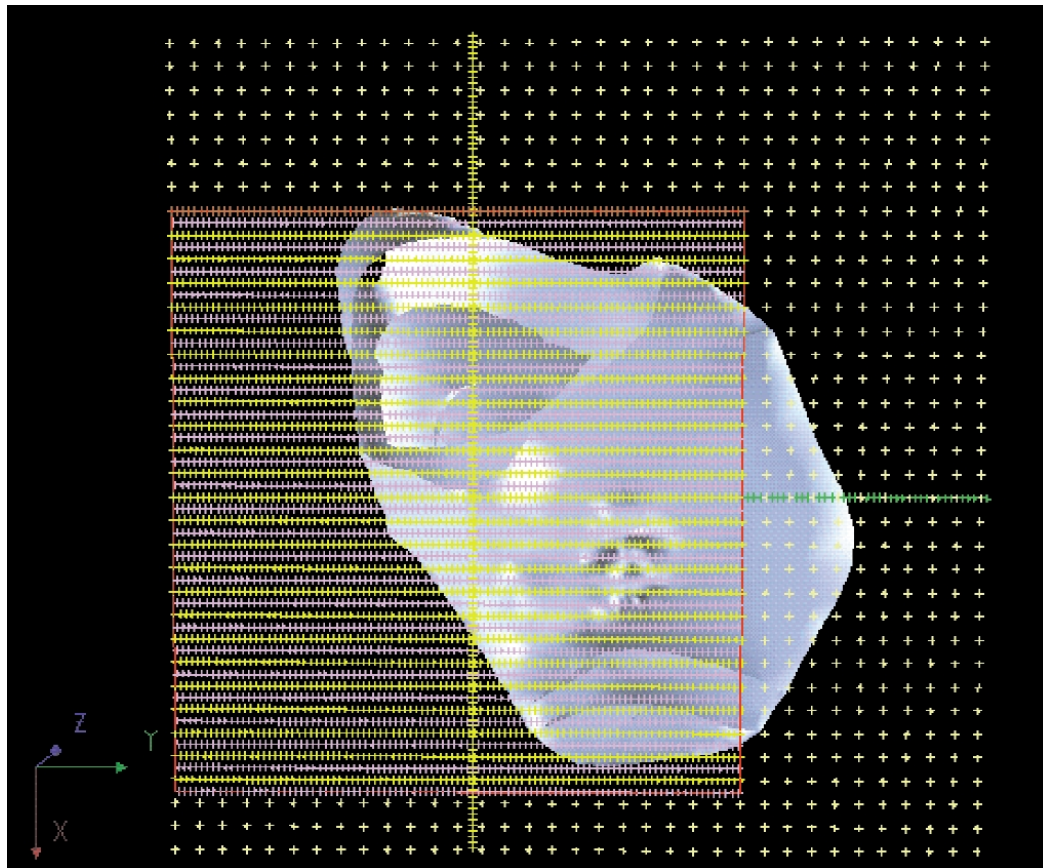


FIGURE 11. Phase B and
Phase C acquisition with an
overlay of phase A lines.

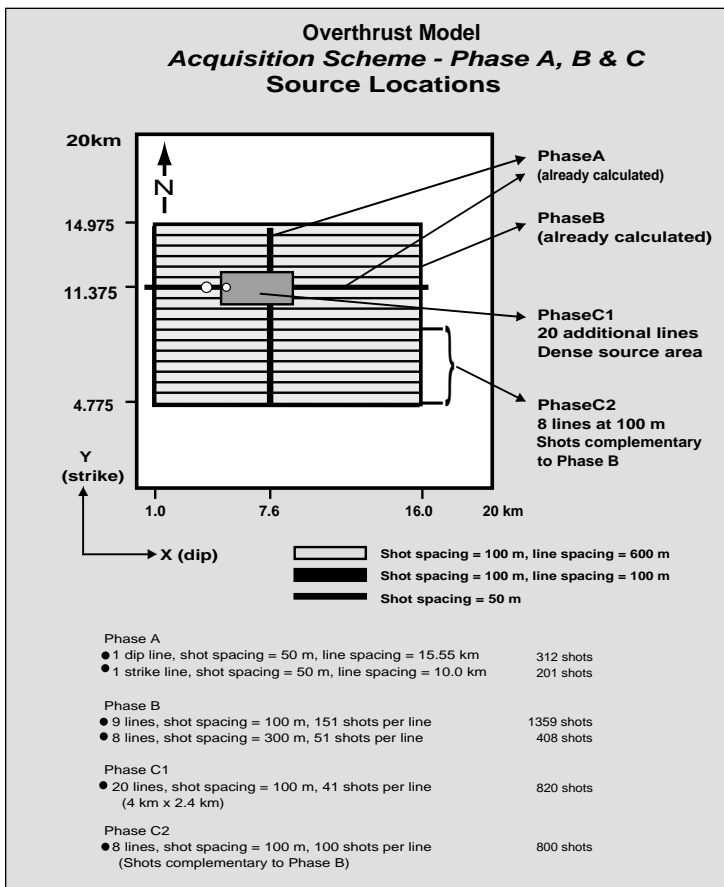


FIGURE 12. Overthrust acquisition for phases A, B, and C.

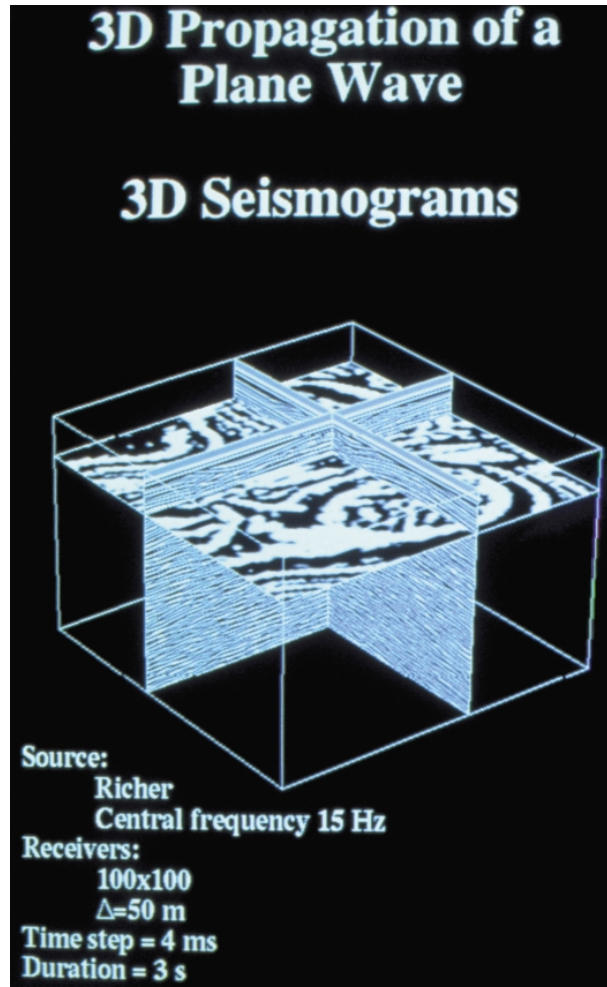


FIGURE 13. Sample 3-D shot for overthrust model.



FIGURE 14. Time slices of wave propagation through the overthrust model.

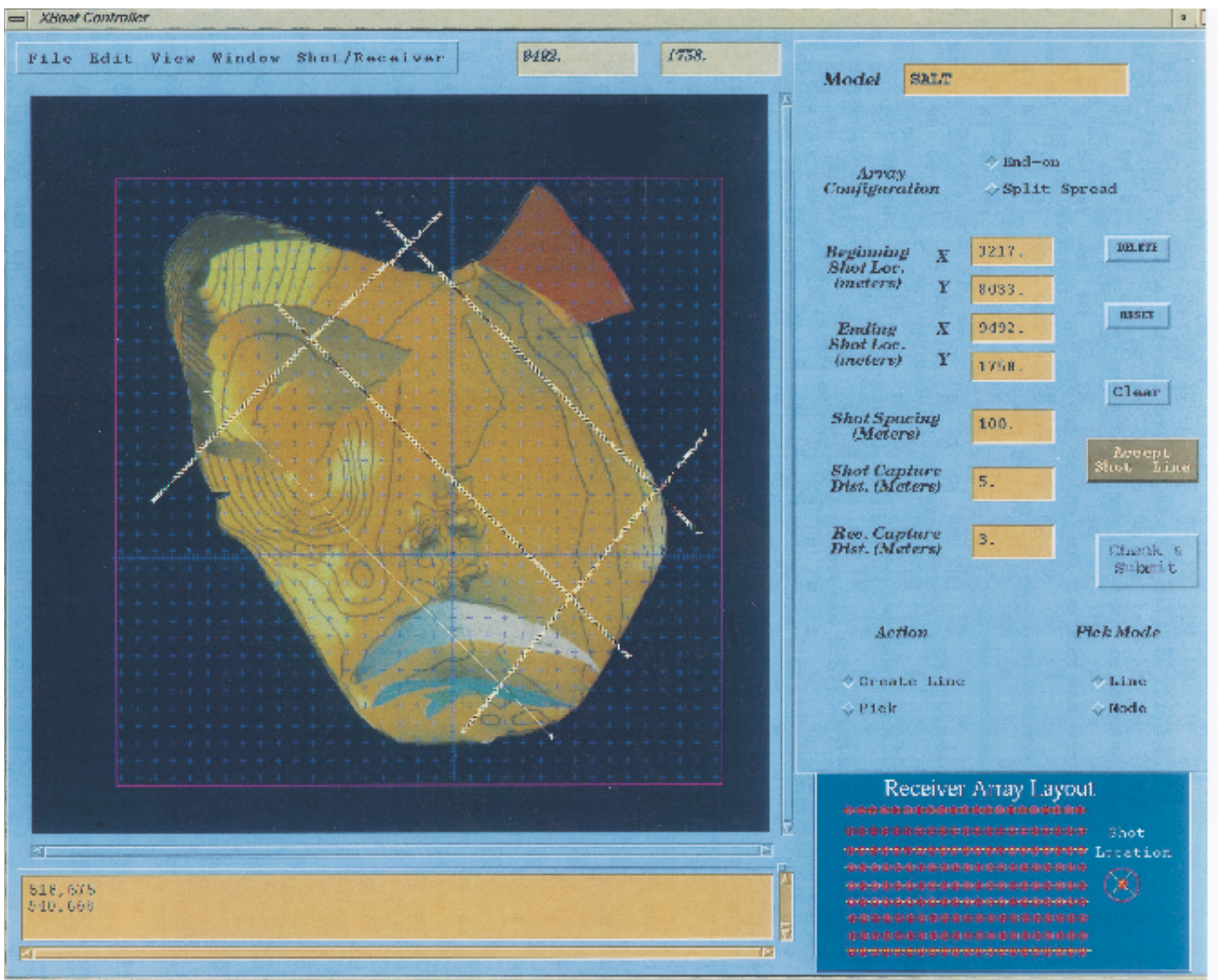


FIGURE 15. A display of the menu-driven program to retrieve desired subsets of the SEMD.

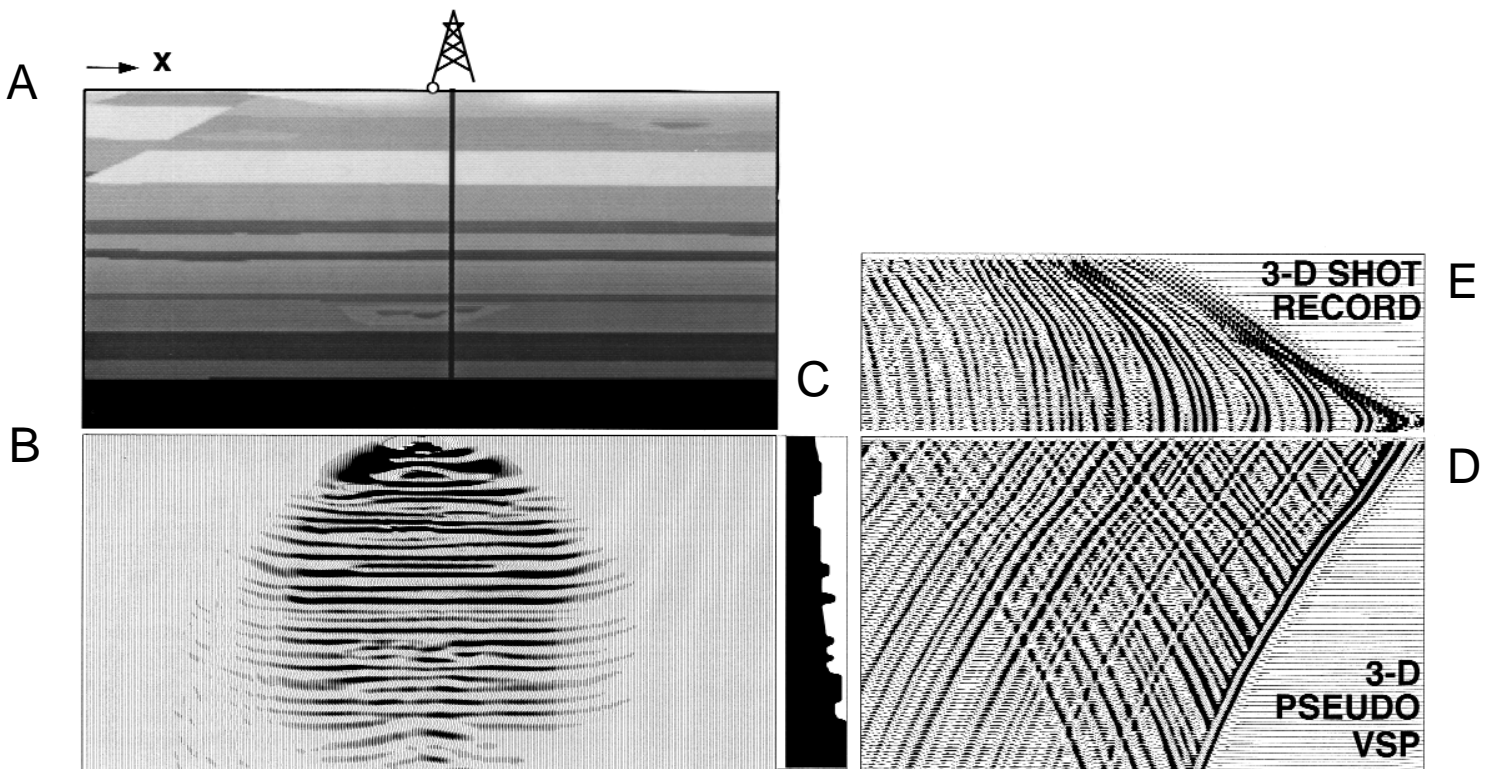


FIGURE 16. Generation of pseudo VSP sections: (A) A 2-D cross section of the overthrust model. (B) 3-D migrated shot record. (C) velocity profile at well location. (D) 3-D pseudo-VSP. (E) 3-D shot record. (From Alai et al., 1995).

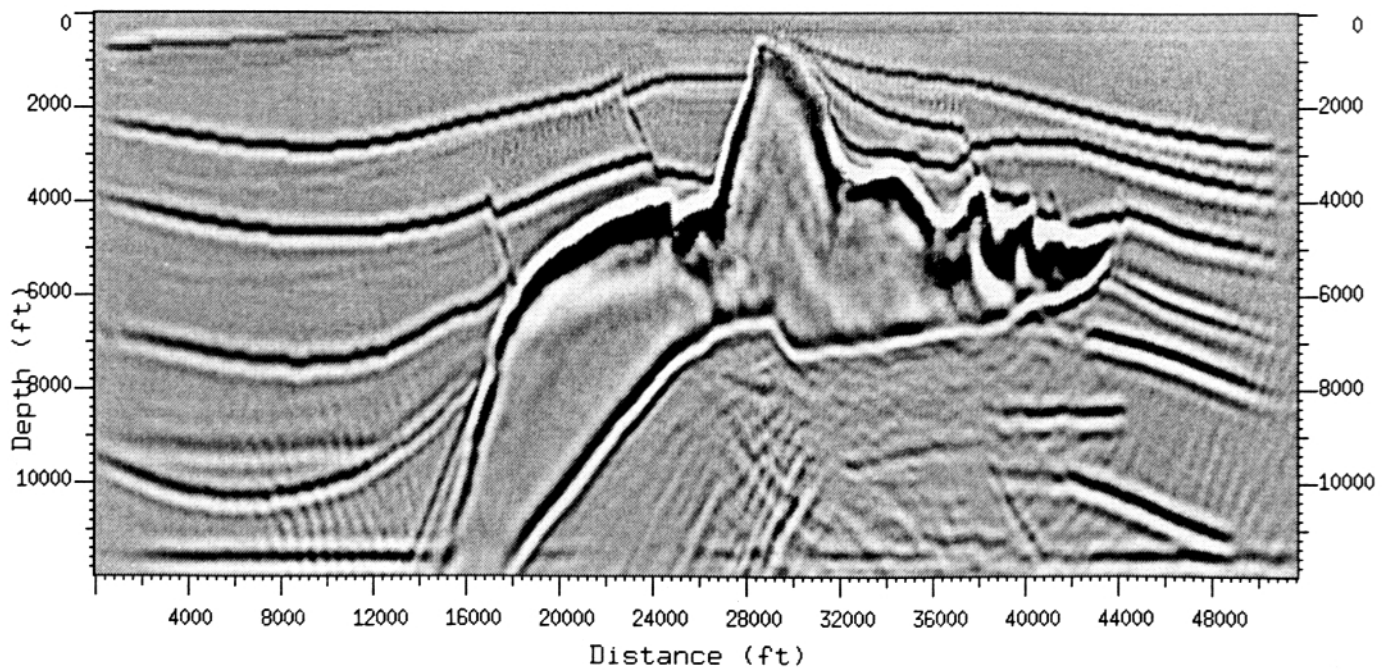


FIGURE 17. Imaging below the salt body after elimination of multiples (from O'Brien and Gray, 1996).

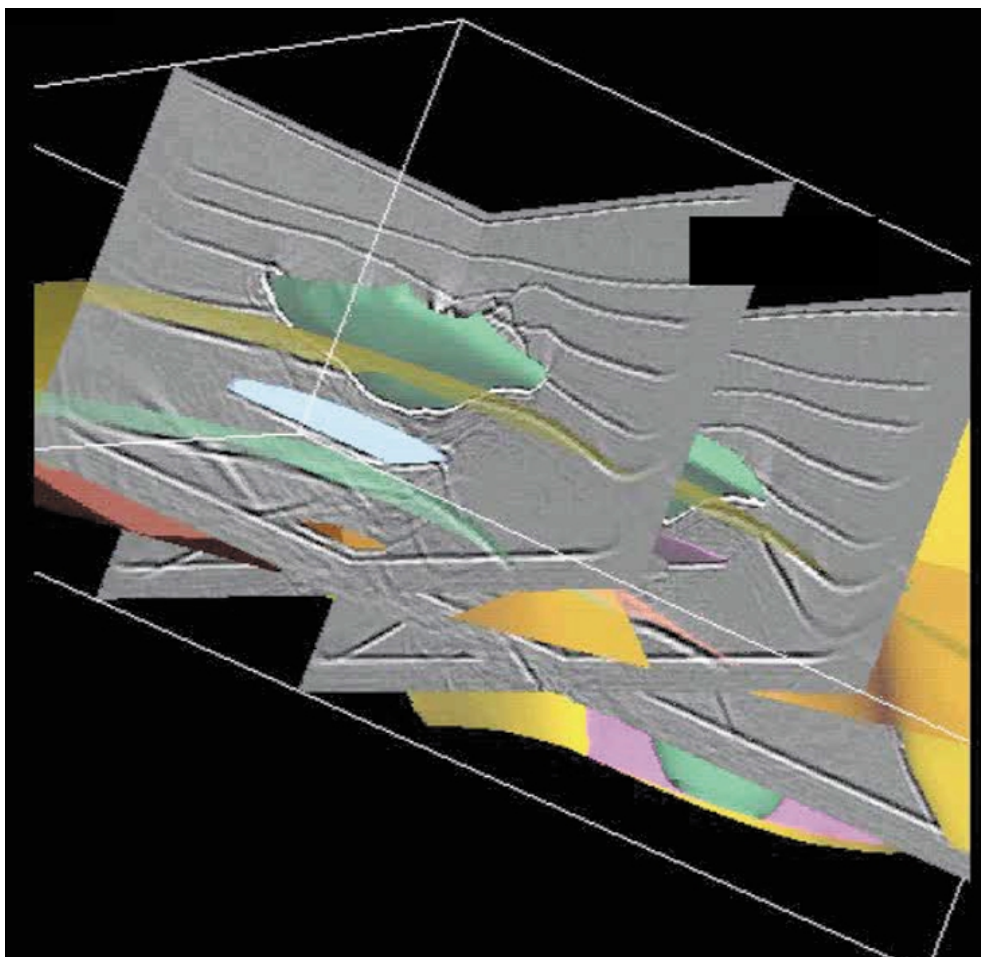


FIGURE 18. 3-D migrated volume overlaid on the 3-D geologic model. (Courtesy of Gulf of Mexico Subsalt Seismic Imaging Project, CRADA LA94C1051.)

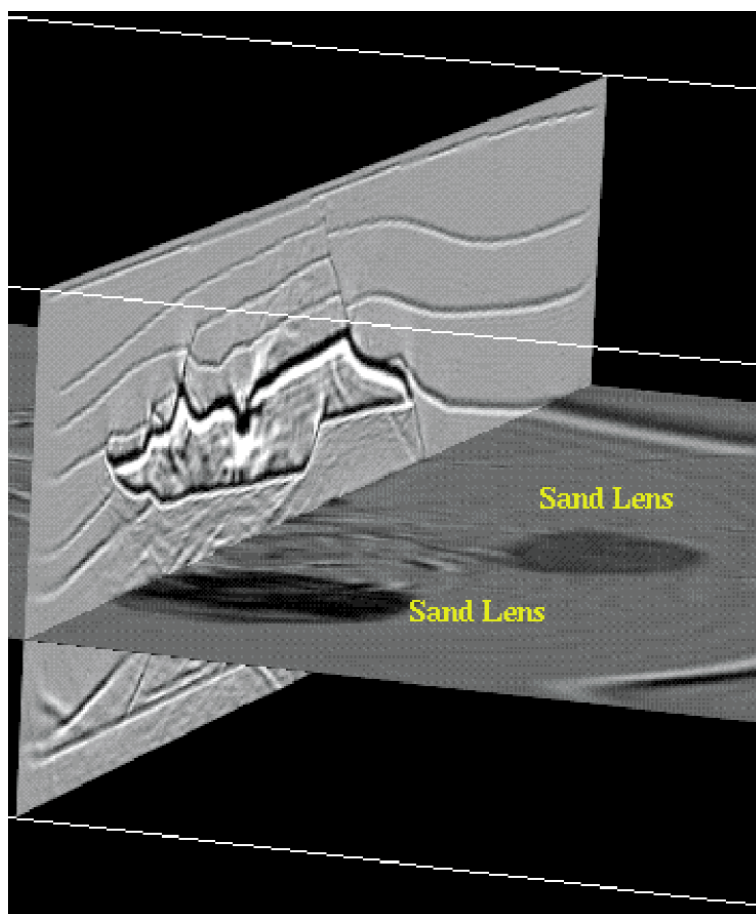


FIGURE 19. Imaged thin sand lens below salt. (Courtesy of Gulf of Mexico Subsalt Seismic Imaging Project, CRADA LA94C1051.)